

Showcasing research from the University of Warwick, UK.

#### Rhodium-catalysed hydrogenation of nitrous oxide

The hydrogenation of nitrous oxide is a thermodynamically favourable transformation relevant to the remediation of this potent greenhouse gas and ozone-depleting substance. Few homogeneous catalysts can operate under the aggressive reaction conditions involved, and our work highlights the potential for molecular complexes of platinum-group metals to decompose into catalytically active nanoparticles.

Image reproduced by permission of Adrian Chaplin from *Catal. Sci. Technol.*, 2025, **15**, 4126.

#### As featured in:



See Adrian B. Chaplin *et al.*,  
*Catal. Sci. Technol.*, 2025, **15**, 4126.



Cite this: *Catal. Sci. Technol.*, 2025, 15, 4126

Received 23rd April 2025,  
Accepted 17th June 2025

DOI: 10.1039/d5cy00490j

rsc.li/catalysis

We report on the discovery of “hidden” heterogeneous catalysis in the hydrogenation of nitrous oxide while assessing the catalytic activity of a rhodium(i) hydride complex supported by a nominally robust phosphine-based pincer ligand. Commercially available  $[\text{Rh}(\text{COD})(\text{OH})]_2$  was subsequently identified as a more effective catalyst precursor, enabling the hydrogenation of nitrous oxide with an apparent turnover number  $>3000$  at room temperature.

Nitrous oxide ( $\text{N}_2\text{O}$ ) is a long-lived gas that accumulates in the atmosphere, contributing to climate change as a potent greenhouse gas and leading to ozone depletion in the stratosphere.<sup>1</sup> Although chemical activation is challenging, exponentially increasing anthropogenic emissions of  $\text{N}_2\text{O}$  make it imperative that energy efficient methods are developed to remediate point sources of this atmospheric pollutant.<sup>2</sup> Direct decomposition into  $\text{N}_2$  and  $\text{O}_2$  is encumbered by the formidable kinetic stability of  $\text{N}_2\text{O}$ , necessitating temperatures  $>700$  °C at atmospheric pressure.<sup>3</sup> While heterogeneous catalysts can promote this reaction (*ca.* 300–600 °C), variants where sacrificial reducing agents are capable of operating at lower temperatures and more appealing from a remediation perspective.<sup>4</sup> In this context, the hydrogenation of  $\text{N}_2\text{O}$  to afford  $\text{N}_2$  and  $\text{H}_2\text{O}$  is a thermodynamically favourable, yet undeveloped transformation, using either heterogeneous or homogeneous catalysts.

Of the limited examples of heterogeneous  $\text{N}_2\text{O}$  hydrogenation described in the literature,<sup>5</sup> the use of platinum group metal catalysts is outstanding for the mild operating temperatures involved. For instance, ruthenium, rhodium,

palladium, and platinum supported on titania promote the hydrogenation of  $\text{N}_2\text{O}$  between 50–150 °C, with activity increasing in the order  $\text{Pd} > \text{Rh} > \text{Pt} > \text{Ru}$  based on measurements made using a flow reactor.<sup>6</sup> Rhodium supported on  $\text{SiO}_2$  and  $\text{Al}_2\text{O}_3$  is also active under flow conditions and a TOF of  $0.022\text{ s}^{-1}$  was measured for the former at 72 °C.<sup>7</sup> Molecular complexes of the platinum group metals have additionally been investigated as homogeneous catalysts, with seminal work using ruthenium pincer complexes reported by Milstein in 2017 (Fig. 1).<sup>8</sup> A mechanism involving O-atom insertion into a Ru-H bond, coupled with bifunctional reactivity of the supporting PNP pincer ligand, was proposed and 417 TONs achieved over 48 h at 65 °C. More productive catalysts have since been identified,<sup>9,10</sup> including a remarkable rhodium-based system by Trincado and Grützmacher, during the preparation of this manuscript, which delivered 230 000 apparent TONs after 96 h at 65 °C (Fig. 1).<sup>11</sup>

Building upon our work with rhodium pincer complexes, which has included the isolation of well-defined  $\text{Rh}-\text{N}_2\text{O}$  adducts,<sup>12</sup> we became interested in assessing the relative catalytic activity of the homologous series of complexes 1–3

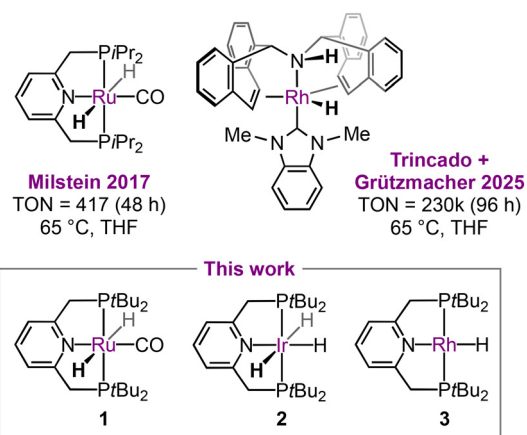


Fig. 1 Late transition metal hydride complexes used as catalysts for the hydrogenation of nitrous oxide.

<sup>a</sup> Department of Chemistry, University of Warwick, Coventry CV4 7AL, UK.  
E-mail: a.b.chaplin@warwick.ac.uk

<sup>b</sup> Department of Physics, University of Warwick, Coventry CV4 7AL, UK

† Electronic supplementary information (ESI) available: Full experimental details, including analysis of catalytic reactions and characterisation of rhodium nanoparticles by TEM/EDX and SAXS. See DOI: <https://doi.org/10.1039/d5cy00490j>



**Table 1** Catalyst screening for the hydrogenation of  $\text{N}_2\text{O}^a$ 

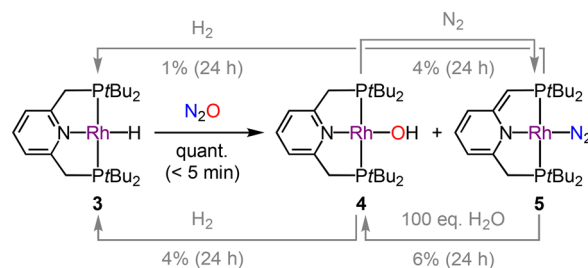
Entry	Catalyst (additive/variation)	[ $\text{H}_2\text{O}$ ]/M	TON
1	None	0.00	—
2	$[\text{Ru}(\text{PNP-}t\text{Bu})\text{HCl}(\text{CO})] (+\text{KO}t\text{Bu})^b$	0.03	5
3	$[\text{Ir}(\text{PNP-}t\text{Bu})\text{H}_3] 2$	0.01	1
4	$[\text{Rh}(\text{PNP-}t\text{Bu})\text{H}] 3^c$	0.90	174
5	$[\text{Rh}(\text{PNP-}t\text{Bu})\text{H}] 3 (+\text{Hg})$	0.01	2
6	$[\text{Rh}(\text{PNP-}t\text{Bu})\text{H}] 3 (\text{THF} \rightarrow \text{CyH})$	<0.01	<1
7	$[\text{Rh}(\text{PNP-}t\text{Bu})\text{OH}] 4^c$	0.75	146
8	$[\text{Rh}(\text{PNP-}t\text{Bu})\text{N}_2] 5^c$	0.75	144
9	$\text{Rh/C}^d$	0.24	47
10	$[\text{Rh}(\text{COD})(\text{OH})]_2 6^c$	1.72	318
11	$[\text{Rh}(\text{COD})(\text{OH})]_2 6 (t = 1 \text{ h})^c$	0.03	6

<sup>a</sup> Conditions: 10  $\mu\text{mol}$  of catalyst/Rh in 2.0 mL of THF placed under  $\sim 1:2 \text{ H}_2/\text{N}_2\text{O}$  (3 atm) within a 100 mL gas bulb with cold finger (126 mL water volume) and stirred at RT for 24 h. Conversion determined by  $^1\text{H}$  NMR analysis using a mesitylene internal standard and averaged over duplicate runs. <sup>b</sup> No conversion observed in the absence of  $\text{KO}t\text{Bu}$ . <sup>c</sup> Generation of  $\text{N}_2$  verified by head space analysis (GC-TCD). <sup>d</sup> Hydrogenation of the internal standard was observed. Similar activity is achieved in the absence of the internal standard.

(Fig. 1). Octahedral hydride complexes **1** (generated from  $[\text{Ru}(\text{PNP-}t\text{Bu})(\text{CO})\text{HCl}]$  and  $\text{KO}t\text{Bu}$ ) and **2** have previously been assessed by Milstein and Suárez,<sup>8,9</sup> and we hypothesised that the component phosphine-based pincer ligand PNP-*t*Bu would be a thermally robust scaffold that would support the homogeneous hydrogenation of  $\text{N}_2\text{O}$  using square-planar rhodium(I) hydride **3**.<sup>13,14</sup>

The hydrogenation of  $\text{N}_2\text{O}$  was first examined at RT using 5 mM solutions of **1–3** in 2.0 mL THF, stirred within the cold finger of a 100 mL gas bulb pressurised with a  $\sim 1:2$  mixture of  $\text{H}_2/\text{N}_2\text{O}$  (3 atm, Table 1). Under these net oxidising conditions, **1** and **2** showed very low catalytic activity, whereas **3** gave 174 apparent TONs over 24 h: as quantified by the formation of water by  $^1\text{H}$  NMR spectroscopy with the generation of  $\text{N}_2$  verified by GC-TCD analysis of the head space.

Encouraged by the high catalytic activity of **3**, we sought to understand the underlying mechanism. To this end, the reaction between **3** (20 mM) and  $\text{N}_2\text{O}$  (2 atm) was examined *in situ* by NMR spectroscopy in  $d^8\text{-THF}$ , revealing quantitative spectroscopic conversion of **3** into a  $\sim 1:1$  mixture of the known rhodium(I) hydroxide complex **4** ( $\delta_{31\text{P}} 55.6$ ,  $^1J_{\text{RhP}} = 162$  Hz) and dearomatized rhodium(I) dinitrogen complex **5** ( $\delta_{31\text{P}} 66.6$ ,  $^1J_{\text{RhP}} = 132$  Hz; 63.1,  $^1J_{\text{RhP}} = 132$  Hz;  $^2J_{\text{PP}} = 269$  Hz) within 5 min at RT (Scheme 1).<sup>15</sup> This outcome is consistent with activation of  $\text{N}_2\text{O}$  by O-atom insertion into the Rh–H bond,<sup>16</sup> followed by (partial) bifunctional elimination of water as proposed for **1** by Milstein.<sup>8</sup> Although independently isolated **4** and **5** are catalytically competent for the hydrogenation of  $\text{N}_2\text{O}$  under the aforementioned conditions (Table 1), they react incomparably slowly with  $\text{H}_2$  at RT on a NMR reaction scale and, moreover, do not reform **3** cleanly (Scheme 1). Likewise, whilst **4** eliminated water to give **5** under an atmosphere of  $\text{N}_2$  and treatment of **5** with excess water gave

**Scheme 1** Reactions of isolated **1–3** in  $d^8\text{-THF}$  at RT.

**4**, both reactions are sluggish at RT and partial decomposition was observed during the former. This decomposition is attributed to the instability of **5** and a significant amount of PNP-*t*Bu oxide was produced when a 20 mM solution of **5** in  $d^8\text{-THF}$  was placed under  $\text{N}_2\text{O}$  (2 atm; 11% after 24 h at RT by  $^{31}\text{P}$  NMR spectroscopy). No reaction with **4** was observed under the same conditions.

These observations, coupled with the deposition of dark residues on the reactor walls and observation of PNP-*t*Bu oxide by  $^{31}\text{P}$  NMR spectroscopy when using **3** in catalysis, led us to question the homogeneous nature of the hydrogenation. The formation of  $2.9 \pm 0.4$  nm rhodium nanoparticles was subsequently confirmed by TEM/EDX analysis of the post-catalysis reaction mixture (Fig. 2A), and their role in catalysis corroborated by a positive mercury drop test, in which addition of mercury almost completely inhibited catalysis using **3** (Table 1, entry 5).<sup>17</sup> The  $\text{N}_2\text{O}$  hydrogenation observed for **3** is therefore not attributed to homogeneous catalysis as we hypothesized, but instead reconciled by the formation of catalytically-active rhodium nanoparticles from partial decomposition of **5** under the reaction conditions (generated from **3** +  $\text{N}_2\text{O}$  or **4** –  $\text{H}_2\text{O}$ , Scheme 1). Isolated **5** displays significantly enhanced stability in cyclohexane and, in further support of this conclusion, **3** is an ineffective catalyst for  $\text{N}_2\text{O}$  hydrogenation when cyclohexane is used in place of THF as the reaction solvent (Table 1, entry 6).

Having concluded that **3** operates *via* heterogeneous catalysis, we sought to identify a more convenient source of rhodium to apply in the hydrogenation of  $\text{N}_2\text{O}$  (Table 1). Commercially available  $\text{Rh/C}$  was first assessed under our conditions but gave only 47 apparent TONs over 24 h. The use of bench stable  $[\text{Rh}(\text{COD})(\text{OH})]_2$  (**6**, COD = 1,5-cyclooctadiene) as a nanoparticle precursor was more promising,<sup>18</sup> with a catalytic turnover nearly double that of **3** recorded after 24 h. Disproportionately low turnover after 1 h is symptomatic of an induction period for **6** and post catalysis analysis of the different runs by SAXS suggests that activity may correlate with a greater degree of nanoparticle aggregation. For instance, particles of mean radius 26.6 nm were observed after 1 h, while after 24 h the scattering data are best modelled as a mixture containing particles with a mean radius of 58.6 nm (see ESI†). These changes in aggregation are also apparent from TEM/EDX analysis of the samples (Fig. 2B/C).



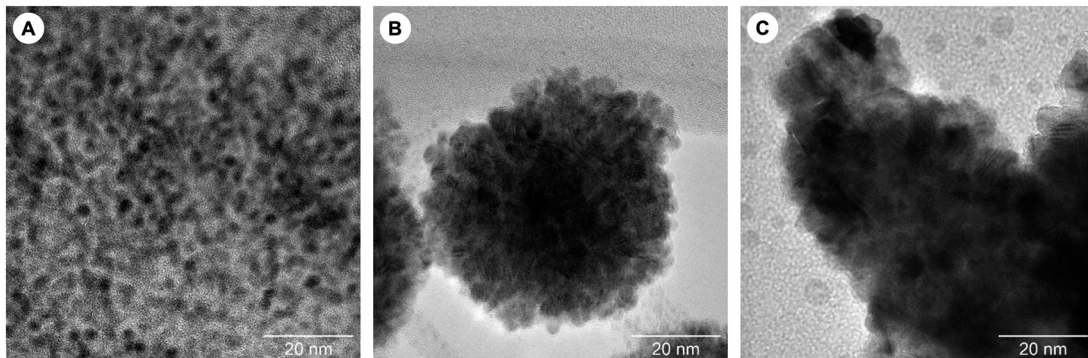


Fig. 2 TEM images taken from post catalysis reaction mixtures when using (A) 3, (B) 6 (1 h run) and (C) 6 (24 h run).

To further explore the catalytic utility of 6, the hydrogenation reaction was tested on a larger scale using a 250 mL gas bulb, under otherwise unoptimised reaction conditions: 5 mM  $[\text{Rh}(\text{COD})(\text{OH})]_2$  in 2.0 mL of THF,  $\sim 1:2$   $\text{H}_2/\text{N}_2\text{O}$  (3 atm). After three successive 24 h cycles, where average cumulative apparent TONs of 982, 2055 and 3261 were measured, a total of 16.3 M of water was produced.

In summary, we have discovered “hidden” heterogenous catalysis in the hydrogenation of  $\text{N}_2\text{O}$  using a rhodium(i) hydride complex featuring a nominally robust phosphine-based pincer ligand. Although reaction with  $\text{N}_2\text{O}$  by O-atom insertion into the Rh-H bond is facile, the ensuing dearomatized rhodium(i) derivative is unstable and partial decomposition into catalytically active rhodium nanoparticles and PNP-*t*Bu oxide was observed during catalysis. Commercially available and bench stable  $[\text{Rh}(\text{COD})(\text{OH})]_2$  was identified as a more effective catalyst precursor, enabling the hydrogenation of  $\text{N}_2\text{O}$  with an apparent turnover number  $>3000$  at RT. We encourage the possible formation of small quantities of catalytically active nanoparticles to be carefully assessed when using molecular catalysts for this reaction.

## Data availability

The data supporting this article have been included as part of the ESI.<sup>†9</sup>

## Conflicts of interest

There are no conflicts to declare.

## Acknowledgements

This work was supported by NERC grants NE/S007350/1 (CENTA2 studentship to SHD) and NE/X018377/1. We also acknowledge funding from the Leverhulme Trust (RPG-2022-214, TMH) and the University of Warwick. TEM and SAXS measurements were made using equipment provided by the University of Warwick Electron Microscopy and X-ray Diffraction Research Technology Platforms.

## Notes and references

- (a) *Climate Change 2023: Synthesis Report*, ed. H. Lee and J. Romero, Intergovernmental Panel on Climate Change, Geneva, Switzerland, 2023, DOI: [10.5932/1pcce/ar6-9789291691647](https://doi.org/10.5932/1pcce/ar6-9789291691647); (b) A. R. Ravishankara, J. S. Daniel and R. W. Portmann, *Science*, 2009, **326**, 123–125.
- H. Tian, R. Xu, J. G. Canadell, R. L. Thompson, W. Winiwarter, P. Suntharalingam, E. A. Davidson, P. Ciais, R. B. Jackson, G. Janssens-Maenhout, M. J. Prather, P. Regnier, N. Pan, S. Pan, G. P. Peters, H. Shi, F. N. Tubiello, S. Zaehle, F. Zhou, A. Arneth, G. Battaglia, S. Berthet, L. Bopp, A. F. Bouwman, E. T. Buitenhuis, J. Chang, M. P. Chipperfield, S. R. S. Dangal, E. Dlugokencky, J. W. Elkins, B. D. Eyre, B. Fu, B. Hall, A. Ito, F. Joos, P. B. Krummel, A. Landolfi, G. G. Laruelle, R. Lauerwald, W. Li, S. Lienert, T. Maavara, M. MacLeod, D. B. Millet, S. Olin, P. K. Patra, R. G. Prinn, P. A. Raymond, D. J. Ruiz, G. R. van der Werf, N. Vuichard, J. Wang, R. F. Weiss, K. C. Wells, C. Wilson, J. Yang and Y. Yao, *Nature*, 2020, **586**, 248–256.
- P. Glarborg, J. E. Johnsson and K. Dam-Johansen, *Combust. Flame*, 1994, **99**, 523–532.
- X. Wu, J. Du, Y. Gao, H. Wang, C. Zhang, R. Zhang, H. He, G. M. Lu and Z. Wu, *Chem. Soc. Rev.*, 2024, **53**, 8379–8423.
- (a) L. Jacobs, C. Barroo, N. Gilis, S. V. Lambeets, E. Genty and T. V. de Bocarmé, *Appl. Surf. Sci.*, 2018, **435**, 914–919; (b) J. Arenas-Alatorre, A. Gómez-Cortés, M. Avalos-Borja and G. Díaz, *J. Phys. Chem. B*, 2005, **109**, 2371–2376; (c) T. Nobukawa, M. Yoshida, K. Okumura, K. Tomishige and K. Kunimori, *J. Catal.*, 2005, **229**, 374–388; (d) A. C. Gluhoi, M. A. P. Dekkers and B. E. Nieuwenhuys, *J. Catal.*, 2003, **219**, 197–205; (e) G. Delahay, M. Mauvezin, A. Guzmán-Vargas and B. Coq, *Catal. Commun.*, 2002, **3**, 385–389; (f) S. A. Carabineiro and B. E. Nieuwenhuys, *Surf. Sci.*, 2001, **495**, 1–7; (g) A. Dandekar and M. A. Vannice, *Appl. Catal., B*, 1999, **22**, 179–200; (h) J. E. Vance and J. K. Dixon, *J. Am. Chem. Soc.*, 1941, **63**, 176–181; (i) J. K. Dixon and J. E. Vance, *J. Am. Chem. Soc.*, 1935, **57**, 818–821; (j) A. F. Benton and C. M. Thacker, *J. Am. Chem. Soc.*, 1934, **56**, 1300–1304; (k) H. Cassel and E. Glückauf, *Z. Phys. Chem.*,



*Abt. B*, 1932, **19**, 47–62; (l) C. N. Hinshelwood, *Proc. R. Soc. London, Ser. A*, 1924, **106**, 292–298.

6 S. Roy, M. S. Hegde, S. Sharma, N. P. Lalla, A. Marimuthu and G. Madras, *Appl. Catal., B*, 2008, **84**, 341–350.

7 (a) N. W. Cant, D. C. Chambers and I. O. Y. Liu, *J. Catal.*, 2011, **278**, 162–166; (b) A. Miyamoto, S. Baba, M. Mori and Y. Murakami, *J. Phys. Chem.*, 1981, **85**, 3117–3122.

8 R. Zeng, M. Feller, Y. Ben-David and D. Milstein, *J. Am. Chem. Soc.*, 2017, **139**, 5720–5723.

9 I. Ortega-Lepe, P. Sánchez, L. L. Santos, P. Lara, N. Rendón, J. López-Serrano, V. Salazar-Pereda, E. Álvarez, M. Paneque and A. Suárez, *Inorg. Chem.*, 2022, **61**, 18590–18600.

10 P. Jurt, A. S. Abels, J. J. Gamboa-Carballo, I. Fernández, G. L. Corre, M. Aebl, M. G. Baker, F. Eiler, F. Müller, M. Wörle, R. Verel, S. Gauthier, M. Trincado, T. L. Gianetti and H. Grützmacher, *Angew. Chem., Int. Ed.*, 2021, **60**, 25372–25380.

11 S. T. Nappen, J. J. Gamboa-Carballo, E. Tschanen, F. Ricatto, M. D. Wörle, A. Thomas, M. Trincado and H. Grützmacher, *Angew. Chem., Int. Ed.*, 2025, **64**, e202502616.

12 M. R. Gyton, B. Leforestier and A. B. Chaplin, *Angew. Chem., Int. Ed.*, 2019, **58**, 15295–15298.

13 L. Schwartsburd, M. A. Iron, L. Konstantinovski, E. Ben-Ari and D. Milstein, *Organometallics*, 2011, **30**, 2721–2729.

14 E. Peris and R. H. Crabtree, *Chem. Soc. Rev.*, 2018, **47**, 1959–1968.

15 (a) S. K. Hanson, D. M. Heinekey and K. I. Goldberg, *Organometallics*, 2008, **27**, 1454–1463; (b) S. M. Kloek, D. M. Heinekey and K. I. Goldberg, *Angew. Chem., Int. Ed.*, 2007, **46**, 4736–4738.

16 (a) T. L. Gianetti, S. P. Annen, G. Santiso-Quinones, M. Reiher, M. Driess and H. Grützmacher, *Angew. Chem., Int. Ed.*, 2016, **55**, 1854–1858; (b) J.-H. Lee, M. Pink, J. Tomaszewski, H. Fan and K. G. Caulton, *J. Am. Chem. Soc.*, 2007, **129**, 8706–8707; (c) A. W. Kaplan and R. G. Bergman, *Organometallics*, 1998, **17**, 5072–5085; (d) A. W. Kaplan and R. G. Bergman, *Organometallics*, 1997, **16**, 1106–1108.

17 (a) R. H. Crabtree, *Chem. Rev.*, 2012, **112**, 1536–1554; (b) J. A. Widgren and R. G. Finke, *J. Mol. Catal. A: Chem.*, 2003, **198**, 317–341.

18 D.-H. Liu, P. M. Pflüger, A. Outlaw, L. Lückemeier, F. Zhang, C. Regan, H. R. Nodeh, T. Cernak, J. Ma and F. Glorius, *J. Am. Chem. Soc.*, 2024, **146**, 11866–11875.

19 (a) S. D. Pike, M. R. Crimmin and A. B. Chaplin, *Chem. Commun.*, 2017, **53**, 3615–3633; (b) B. Gnanaprakasam, J. Zhang and D. Milstein, *Angew. Chem., Int. Ed.*, 2010, **49**, 1468–1471; (c) A. van der Ent, A. L. Onderdelinden and R. A. Schunn, *Inorg. Synth.*, 1990, **28**, 90–92; (d) D. Hermann, M. Gandelman, H. Rozenberg, L. J. W. Shimon and D. Milstein, *Organometallics*, 2002, **21**, 812–818; (e) M. R. Gyton, T. M. Hood and A. B. Chaplin, *Dalton Trans.*, 2019, **48**, 2877–2880; (f) E. M. Pelczar, T. J. Emge, K. Krogh-Jespersen and A. S. Goldman, *Organometallics*, 2008, **27**, 5759–5767; (g) R. Uson, L. A. Oro, J. A. Cabeza, H. E. Bryndza and M. P. Stepro, *Inorg. Synth.*, 1985, **23**, 126–130; (h) P. S. Pregosin, *NMR in Organometallic Chemistry*, Wiley-VCH, 2012, pp. 251–254; (i) XSACT: X-ray scattering, analysis, and calculation tool (Xenocs, version 2.7), 2023; (j) J. Ilavsky and P. R. Jemian, *J. Appl. Crystallogr.*, 2009, **42**, 347–353; (k) W. Li, J.-H. Xie, H. Lin and Q.-L. Zhou, *Green Chem.*, 2012, **14**, 2388–2390; (l) L. R. Doyle, A. Heath, C. H. Low and A. E. Ashley, *Adv. Synth. Catal.*, 2014, **356**, 603–608.

